Cell, Vol. 86, 59–69, July 12, 1996, Copyright ©1996 by Cell Press

LIM-kinase1 Hemizygosity Implicated in Impaired Visuospatial Constructive Cognition

J. Michael Frangiskakis,[1,2] Amanda K. Ewart,[1,2] Colleen A. Morris,[6] Carolyn B. Mervis,[7] Jacquelyn Bertrand,[7] Byron F. Robinson,[7] Bonita P. Klein,[7] Gregory J. Ensing,[8] Lorraine A. Everett,[9] Eric D. Green,[9] Christoph Pröschel,[5] Nick J. Gutowski,[10] Mark Noble,[5] Donald L. Atkinson,[1,2,3] Shannon J. Odelberg,[1,2] and Mark T. Keating[1,2,3,4]

[1]Department of Human Genetics
[2]Eccles Institute of Human Genetics
[3]Howard Hughes Medical Institute
[4]Cardiology Division
[5]Huntsman Cancer Institute
Department of Oncological Sciences
University of Utah Health Sciences Center
Salt Lake City, Utah 84112
[6]Departments of Pediatrics and Pathology
and Laboratory Medicine
University of Nevada School of Medicine
Las Vegas, Nevada 89102
[7]Department of Psychology
Emory University
Atlanta, Georgia 30322
[8]Department of Pediatrics
Division of Pediatric Cardiology
Indiana University School of Medicine
Indianapolis, Indiana 46202
[9]National Center for Human Genome Research
National Institutes of Health
Bethesda, Maryland 20892
[10]Department of Clinical Neurology
Institute of Neurology
Queen Square, London
United Kingdom

Summary

To identify genes important for human cognitive development, we studied Williams syndrome (WS), a developmental disorder that includes poor visuospatial constructive cognition. Here we describe two families with a partial WS phenotype; affected members have the specific WS cognitive profile and vascular disease, but lack other WS features. Submicroscopic chromosome 7q11.23 deletions cosegregate with this phenotype in both families. DNA sequence analyses of the region affected by the smallest deletion (83.6 kb) revealed two genes, *elastin* (*ELN*) and *LIM-kinase1* (*LIMK1*). The latter encodes a novel protein kinase with LIM domains and is strongly expressed in the brain. Because *ELN* mutations cause vascular disease but not cognitive abnormalities, these data implicate *LIMK1* hemizygosity in impaired visuospatial constructive cognition.

Introduction

The ability to visualize an object (or picture) as a set of parts and construct a replica of the object from those parts is known as visuospatial constructive cognition. Neuroanatomical studies in humans and animals suggest that neurons in the posterior parietal cortex are critical for this process (Capruso et al., 1995). This cognitive function is likely mediated by a network of neurons capable of parallel processing. The molecular mechanisms underlying development of these networks, however, are not understood.

Williams syndrome (WS) is a complex developmental disorder that includes a specific cognitive profile (WSCP) characterized by relative strength in language and auditory rote memory and pronounced weakness in visuospatial constructive cognition (Udwin et al., 1987; Morris et al., 1988; Dilts et al., 1990; Bellugi et al., 1994; Mervis and Bertrand, 1996; Mervis et al., 1996). Additional features of WS include congenital heart and vascular disease, dysmorphic facial features, infantile hypercalcemia, mental retardation, and a characteristic personality. Most individuals with WS have mild or moderate mental retardation (mean IQ ranging from 55–60), but some have borderline normal intelligence or severe mental retardation. This combination of features results in a remarkable phenotype readily distinguished from other disorders involving mental retardation. The incidence of WS is estimated to be 1 in 20,000 live births.

The visuospatial constructive cognitive deficit observed in WS is best demonstrated by tasks involving pattern construction. Performance of these tasks depends on the ability of an individual to see an object in terms of a set of parts and use those parts to construct a replica of the pictured object. Specifically, individuals are shown a picture of a block design and must construct the corresponding pattern using cubes of varying colors and designs. Individuals with WS typically have difficulty constructing even simple patterns, such as a checkerboard consisting of four cubes. As a result, individuals with WS have marked difficulty in tasks involving the use of a pattern to assemble an object (e.g., building a model or assembling a simple piece of furniture).

Approximately 77% of individuals with WS have clinically apparent supravalvular aortic stenosis (SVAS), an obstructive vascular disease (Lowery et al., 1995). SVAS can be inherited as part of WS or as an isolated, autosomal dominant trait (Curran et al., 1993; Ewart et al., 1993b, 1994; Morris et al., 1993). SVAS may be associated with some connective tissue abnormalities seen in WS, but other WS features are not observed. In particular, autosomal dominant SVAS is not associated with impaired visuospatial constructive cognition. Recently, we used genetic linkage and mutational analyses to show that mutations in *elastin* (*ELN*) cause autosomal dominant SVAS (Ewart et al., 1993a, 1994; Curran et al., 1993; Morris et al., 1993). Known SVAS-causing mutations in *ELN* include a translocation, an intragenic deletion, and missense and nonsense mutations (Curran et al., 1993; Olson et al., 1995; unpublished data).

Because there is a phenotypic link between SVAS and WS, we hypothesized that mutations involving *ELN* might also contribute to WS. We discovered that WS

results from submicroscopic deletions of chromosome 7q11.23 (Ewart et al., 1993a). Inherited or de novo deletion of one *ELN* allele was identified in 239 of 240 WS individuals (Ewart et al., 1993a; Lowery et al., 1995; unpublished data). These data indicate that *ELN* mutations cause isolated, autosomal dominant SVAS and that hemizygosity at the *ELN* locus is responsible for vascular pathology in WS. *ELN* hemizygosity may also account for some connective tissue abnormalities observed in individuals with autosomal dominant SVAS or WS, including premature aging of skin, some WS facial features, diverticulosis of the bladder and colon, hoarse voice, hernias, and joint abnormalities. *ELN* mutations, however, do not account for all WS features and are not the cause of impaired visuospatial constructive cognition. Because genomic deletions responsible for WS extend well beyond the *ELN* locus (unpublished data), we have hypothesized that WS is a contiguous gene deletion syndrome (Ewart et al., 1993a).

Here, we report identification and characterization of two families with a partial WS phenotype consisting of SVAS, some WS facial features, and impaired visuospatial constructive cognition, but lacking other features of this disorder. Affected family members harbor smaller chromosomal deletions (83.6 and ~300 kb) than those identified in individuals with classic WS (>500 kb), an observation that supports the hypothesis that WS is a contiguous gene deletion syndrome (Ewart et al., 1993a; Gilbert-Dussardier et al., 1995). DNA sequence analyses of the 83.6 kb deletion region revealed two genes, *ELN* and *LIM-kinase1* (*LIMK1*; Mizuno et al., 1994; Bernard et al., 1994). No other genes were identified in the region. Northern blot and in situ hybridization analyses indicate that *LIMK1* is strongly expressed in discrete regions of the brain. Because *ELN* mutations cause vascular disease but not cognitive abnormalities, these data indicate that *LIMK1* hemizygosity contributes to impaired visuospatial constructive cognition in WS.

Results

Identification of Individuals with a Partial WS Phenotype

To test the hypothesis that WS is a contiguous gene deletion syndrome, we sought to identify individuals with a partial WS phenotype. We characterized people with SVAS for the presence of additional WS features, including facial appearance, WSCP, and mental retardation. Phenotypic studies included personal interview, physical examination, two-dimensional and Doppler echocardiography, IQ determination, and WSCP analyses.

Phenotypic assignment with respect to WSCP was based, whenever possible, on the pattern of performance on subscales of the Differential Ability Scales (DAS; Elliott, 1990), a standardized measure of cognitive abilities. When the DAS could not be administered, phenotypic assignment was based on performance on subscales of the Wechsler Adult Intelligence Scale-Revised (WAIS-R; Wechsler, 1981), the Developmental Test of Visual Motor Integration (VMI; Beery, 1989), or the Mental Scale of the Bayley Scales of Infant Development (Bayley; Bayley, 1969, 1993). Use of the Bayley to determine whether the cognitive profile of a child is consistent with the WSCP has been validated in a study comparing very young children with WS to very young children with Down's syndrome (Mervis and Bertrand, 1996). In the present study, the Bayley measure was used for only one child (K1895 II-4), who was 15 months old at the time of assessment. Quantitative data from the DAS, WAIS-R, or Bayley were used to test for the presence of WSCP, which involves a weakness in pattern construction and a strength in digit recall relative to performance on other subtests (Tables 1–3).

To determine the sensitivity of WSCP assessment, the DAS was also administered to 48 individuals with WS ranging in age from 4 to 47 years (IQ range 35–84). Of these individuals, 45 fit the WSCP; 40 had an excellent fit, 3 had a very good fit, and 2 had a good fit. To determine specificity, we also examined the performance of 25 control individuals with below average IQ (IQ range 30–95). Some of these controls had other syndromes (e.g., Down's syndrome or Fragile X syndrome); the others had no specific diagnosis. Of these individuals, 23 of 25 definitely did not fit the WSCP. Thus, the WSCP measure has excellent sensitivity (.94) and specificity (.92).

Phenotypic characterization of individuals with isolated, autosomal dominant SVAS indicated that these individuals did not manifest the other major features of WS (Table 1; data not shown). Occasionally, an individual with autosomal dominant SVAS presented with a few WS facial features ($\leq$6 of 16) or a hernia (or both), but no other WS phenotypic characteristics were observed. In particular, no one with autosomal dominant SVAS showed evidence of WSCP. Because these individuals harbor a mutation (translocation or point mutation) that disrupts one *ELN* allele, these data indicate that *ELN* mutations cause vascular disease but not impaired visuospatial constructive cognition.

Continued ascertainment and phenotypic characterization revealed two families with a partial WS phenotype (Figure 1). Most affected members of these families had SVAS, some WS facial features, and WSCP. These individuals showed levels of verbal ability and auditory short-term memory similar to those of unaffected family members, but their visuospatial constructive abilities were markedly impaired. Affected members lacked other WS features (Table 1). Serum calcium levels during infancy were available for only four individuals, but none showed evidence of hypercalcemia (data not shown). No WS phenotypic characteristics were present in unaffected family members.

Previous studies indicated marked intra- and interfamilial variability of expression and incomplete penetrance for autosomal dominant SVAS (Curran et al., 1993; Ewart et al., 1993b, 1994; Morris et al., 1993). We found similar variability among individuals with partial WS phenotypes. For example, SVAS was severe and required surgery in two members of K2049 (individuals III-3 and III-7) and led to early death in three members of K1895 (individuals not shown on pedigree). Other affected members of these kindreds exhibited mild to moderate SVAS, and vascular disease was not clinically apparent in two members of K2049 (individuals II-3 and III-2).

Table 1. Phenotypic Evaluation of Individuals with Partial WS Phenotype and Control Subjects

Individual	SVAS	Facies	WSCP	MR/DD	Deletion
K1895					
I-2	+	3	+	−	D (~300 kb)
I-3	−	0	−	−	N
II-1	−	0	−	−	N
II-2	+	5	+	−	D (~300 kb)
II-3	−	0	−	−	N
II-4	+	2	+	−	D (~300 kb)
II-5	−	0	−	−	N
II-6	−	0	−	−	N
K2049					
I-1	+	4	+	−	D (83.6 kb)
II-2	+	2	+	−	D (83.6 kb)
II-3	−	2	+	−	D (83.6 kb)
II-4	+	0	+	−	D (83.6 kb)
II-5	−	0	−	−	N
II-6	+	4	+	−	D (83.6 kb)
II-7	−	0	−	−	N
III-1	−	0	−	−	N
III-2	−	0	+	−	D (83.6 kb)
III-3	+	0	U	−	D (83.6 kb)
III-4	−	0	−	−	N
III-5	−	0	−	−	N
III-6	+	0	+	+	D (83.6 kb)
III-7	+	0	−	−	D (83.6 kb)
III-8	−	0	−	−	N
IV-1	−	0	−	−	N
IV-2	+	6	+	−	D (83.6 kb)
Classic WS					
13759	+	13	+	+	D (>500 kb)
13946	+	16	+	+	D (>500 kb)
14033	+	15	+	+	D (>500 kb)
14101	+	13	+	+	D (>500 kb)
14576	−	14	+	+	D (>500 kb)
15083	+	13	+	+	D (>500 kb)
15266	+	13	+	+	D (>500 kb)
17402	+	13	+	+	D (>500 kb)
18031	−	14	+	+	D (>500 kb)
18296	+	14	+	+	D (>500 kb)
Autosomal Dominant SVAS					
12903	+	1	−	−	N
12905	+	3	−	−	N
12906	+	2	−	−	N
12907	+	0	−	−	N
13222	+	1	−	−	N
13835	+	0	−	−	N
14104	+	1	−	−	N
14107	+	0	−	−	N
17607	+	2	−	−	N
20583	+	2	−	−	N

Phenotypic evaluation was completed in members of two families with a partial WS phenotype (K1895 and K2049), individuals with classic WS, and individuals with autosomal dominant SVAS resulting from *ELN* mutations. Phenotypic assignments included the presence (plus) or absence (minus) of SVAS, WSCP, and mental retardation or developmental delay (MR/DD). The number of WS facial features present (Facies) is also indicated (0–16 of 16 possible WS facial features). The phenotypic assessments for WSCP were based on numerical scores obtained from the DAS, WAIS-R, or Bayley. Individual III-3 of K2049 was characterized as phenotypically uncertain (U) with respect to WSCP because of a seizure disorder treated with anti-convulsant medication. Individual III-6 had mild developmental delay, with an IQ of 64; the 95% confidence interval was 58–71 (an IQ score of ≥70 would be in the normal range). The presence (D) or absence (N) of a chromosome 7q11.23 deletion is indicated at right. Note that SVAS, mild WS facial features, and the WSCP cosegregated with deletions in K1895 and K2049. Incomplete penetrance and variable expression were apparent in these kindreds.

Some WS facial features (2–6 of 16) were observed in all affected members of K1895 and in 5 of 10 affected members of K2049, but these features did not fulfill the criteria for WS (9 of 16 facial features). WSCP was observed in all affected members of K1895 and in 8 of 10 affected members of K2049. These phenotypic studies indicate autosomal dominant coinheritance of SVAS, some WS facial features, and WSCP in two families with variable phenotypic expression and incomplete penetrance. Identification of individuals with a partial WS phenotype supports the hypothesis that WS is a contiguous gene deletion syndrome.

Table 2. Assessment of WSCP for Individuals Completing the DAS

	Exclusion			Strength of Fit to WSCP		
Individual	PC ≥ T	PC ≥ D	PC ≥ 20%	D > T	V > PC	Total
K1895						
I-2				2	2	4
I-3		X				
II-1	X	X				
II-2				2	2	4
II-3	X		X			
II-5	X		X			
II-6	X	X	X			
K2049						
III-1	X		X			
III-2				2	2	4
III-4	X					
III-5		X				
III-6				2	2	4
III-7		X				
III-8	X	X				
IV-1			X			
IV-2				2	2	4
Classic WS						
13759				2	2	4
13946				2	2	4
14033				2	2	4
14101				2	2	4
14576				2	2	4
15083				2	2	4
15266				2	2	4
17402				2	2	4
18031				2	2	4
18296				2	2	4
Autosomal dominant SVAS						
12903	X	X	X			
12905	X	X	X			
12906			X			
12907	X		X			
13222	X	X	X			
13835	X	X	X			
14104	X	X	X			
14107	X	X	X			
17607	X	X	X			
20583	X	X	X			
Normal						
29999		X	X			
29998	X		X			

WSCP evaluation using the DAS was completed in members of K1895 and K2049, individuals with classic WS, individuals with autosomal dominant SVAS, and normal controls. DAS evaluation included assessment of pattern construction (PC), digit recall (D), verbal abilities (V), and mean standard score for the core subtests (T). The WSCP was excluded if PC ≥ T, PC ≥ D, or PC ≥ 20th percentile. For individuals who were not excluded, level of fit to the WSCP was based on total score: 0–1 point, poor fit; 2, good fit; 3, very good fit; 4, excellent fit.

Association of Partial WS Phenotypes with Submicroscopic Chromosome 7q11.23 Deletions

We constructed a contiguous physical map comprised of cosmids and phage that span ~107 kb of chromosome 7q11.23, including the entire *ELN* locus (Figure 2). To determine whether individuals with a partial WS phenotype carried smaller deletions, we performed fluorescence in situ hybridization (FISH) using cosmids that span the *ELN* locus. All affected members of K1895 showed *ELN* hemizygosity, while unaffected members had two *ELN* alleles. Additional FISH analyses revealed hemizygosity with probes c138-13c and c1-4a2 (data not shown). These results indicated that affected members of K1895 harbor a deletion in chromosome 7q11.23 that includes *ELN*. FISH analyses using yeast artificial chromosomes (YACs) from this region indicate a deletion of ~300 kb (unpublished data). By contrast, analyses of individuals with classic WS indicate that these deletions span more than 500 kb (unpublished data).

We previously described a deletion associated with SVAS in two members of K2049 (Ewart et al., 1994). Oligonucleotides flanking the deletion breakpoints were used to define a novel polymerase chain reaction (PCR) product of 403 bp observed only in phenotypically affected kindred members (Figure 1B). Physical mapping and restriction analyses revealed an ~85 kb deletion (Figure 2), much smaller than that observed in classic WS (≥500 kb). These data indicate that a partial WS phenotype, including SVAS, some WS facial features,

Table 3. Assessment of WSCP for Individuals Who Did Not Complete the DAS

Individuals Who Completed the WAIS-R					
	Exclusion		Inclusion		
Individual	PC ≥ D	PC ≥ 20%	D > PC	V > PC	WSCP
K2049					
I-1			[a]	+	+
II-2			+	+	+
II-3			+	+	+
II-4			+	+	+
II-5	+				−
Individuals Who Completed the Verbal WAIS-R and the VMI					
	Exclusion		Inclusion		
Individual	VMI AE > 10 years		Verbal WAIS-R > VMI		WSCP
K2049					
II-6			+		+
II-7	+				−
Individual Who Completed the Bayley					
	Bayley I		Bayley II		
Individual	%LI > %NLI		%LI > %NLI		WSCP
K1895					
II-4	+		+		+

Adults who could not complete the DAS were phenotypically characterized with the WAIS-R whenever possible. Phenotypic characterizations based on the WAIS-R included assessments of pattern construction (PC; block design subtest), digit recall (D), and verbal abilities (V). Inclusion criteria for Bayley I and Bayley II were based on passing a greater proportion of language items attempted (%LI) than nonlanguage items attempted (%NLI). Individuals II-6 and II-7 of K2049 only completed the verbal portion of the WAIS-R, so additional characterization was completed using the Developmental Test of Visual Motor Integration (VMI). VMI AE, age equivalent for the VMI. Individual II-4 of K1895 was too young to complete the DAS, so phenotypic characterization was carried out using the Bayley test.

[a] Digit recall assessment was inappropriate owing to dementia.

and WSCP, cosegregates with the ~85 kb deletion in this family. Because intragenic mutations of *ELN* cause isolated SVAS and some WS facial features (Curran et al., 1993; Morris et al., 1993; Olson et al., 1995), but not WSCP (Table 1), a gene responsible for the impaired visuospatial constructive cognition must be located immediately 3′ of *ELN*.

Identification of a Protein Kinase Gene Immediately 3′ of *ELN*

We tested the specific hypothesis that hemizygosity of a gene encoding a protein kinase could cause impaired visuospatial constructive cognition. This hypothesis was based on observations that targeted disruption of genes encoding protein kinases results in mice with impaired spatial learning (Grant et al., 1992; Abeliovich et al., 1993a, 1993b). We designed oligonucleotides complementary to sequences conserved in tyrosine kinases and performed PCR analyses with genomic clones from the physical map. A specific product of 315 bp was identified from cosmid c138-13c. This PCR product was cloned; DNA sequence analyses revealed an open reading frame of 113 nt with complete homology to *LIMK1*, a recently identified gene encoding a protein kinase with LIM domains (Mizuno et al., 1994; Bernard et al., 1994). Oligonucleotides based on published cDNA sequences were used in PCR experiments to clone *LIMK1* cDNA from a human hippocampal cDNA library. PCR analyses of DNA from somatic cell hybrids, cosmids, P1s, and YACs localized *LIMK1* to the deleted region on chromosome 7q11.23. These data place *LIMK1* immediately 3′ of *ELN* and within the ~85 kb deletion identified in K2049.

Cosegregation of *LIMK1* Hemizygosity and Impaired Visuospatial Constructive Cognition

To test the hypothesis that *LIMK1* hemizygosity contributes to the WSCP, we performed FISH analyses with metaphase chromosomes from individuals with both partial and classic WS phenotypes using cosmids cELN-11d, c138-13c, and c1-4a2. *LIMK1* was completely deleted from one chromosome 7 homolog in affected members of K1895 and K2049 and in 62 of 62 individuals with classic WS (data not shown). *LIMK1* was not deleted in 6 of 6 individuals with autosomal dominant and de novo SVAS or in more than 100 control individuals (data not shown). These data indicate that *LIMK1* is deleted in individuals with classic and partial WS, but not in individuals with autosomal dominant SVAS and suggest that *LIMK1* hemizygosity contributes to WSCP.

Only *ELN* and *LIMK1* Are Identified by DNA Sequence Analyses of the ~85 kb Deletion Region

To determine whether *LIMK1* is the only gene from this region likely to contribute to cognitive development, we sequenced the ~85 kb segment deleted in K2049, along with flanking sequences. DNA sequence analyses defined two ordered contigs of 41,566 and 65,607 bp separated by a gap of ~250 bp (Figure 2). We were unable to sequence this gap, because of high GC content.

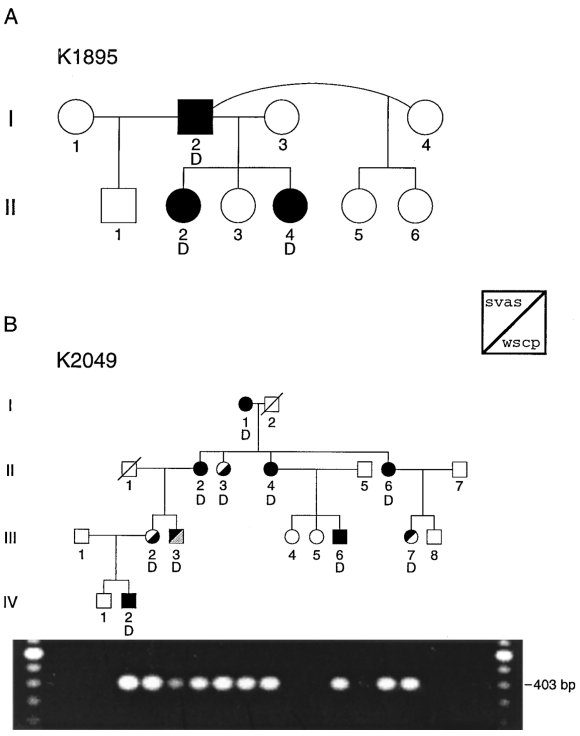

Figure 1. Coinheritance of a Partial WS Phenotype and Deletions Involving *ELN* and *LIMK1* in Kindreds 1895 and 2049

Individuals with SVAS are indicated by closed upper half-circles (females) or squares (males). Individuals with the WSCP are indicated by closed lower half-circles or squares. Individuals with SVAS and WSCP are indicated by completely closed circles and squares; phenotypically unaffected individuals are indicated by open symbols.

(A) Pedigree structure and phenotypic assignments for K1895 are shown. Individuals I-2, II-2, and II-4 were phenotypically affected with both SVAS and WSCP. No features of WS were identified in other members of this kindred. Individuals harboring an ~300 kb deletion of chromosome 7q11.23, including the entire *ELN* and *LIMK1* genes, are indicated by a D. Note that this deletion cosegregates with the SVAS/WSCP phenotype in this family.

(B) Phenotypic designations for members of K2049 are as described above, except that an uncertain phenotype is indicated by stippling. Oligonucleotide primers 403f and 403r were used to define a novel 403 bp PCR product that spans the 83.6 kb deletion in affected members of this family. The results of PCR analyses are shown below in the lane corresponding to each symbol. Note that this 83.6 kb deletion cosegregates with SVAS/WSCP in this family but penetrance is incomplete.

These data indicated that the segment deleted in K2049 spans 83.6 kb. Restriction maps predicted from DNA sequence analyses were identical to maps generated using BamHI, EcoRI, and HindIII. The sequences were analyzed for the presence of known genes using the GRAIL, GENQUEST, and BLAST servers (Xu et al., 1994; Altschul et al., 1990); only *ELN* and *LIMK1* were detected.

Comparison between the cDNA and genomic sequence revealed 16 *LIMK1* exons that span 37 kb of genomic DNA. Sequence analyses also indicated that *LIMK1* is located 15.4 kb 3′ of *ELN* (Figure 2). Predicted amino acid sequence analyses identified all previously described domains, including LIM-1, LIM-2, a Dlg homology region, a putative nuclear localization signal, and a kinase domain (Mizuno et al., 1994; Ponting and Phillips, 1995). In addition, our sequence analyses revealed a possible PEST domain (PESTFIND score of 6.3; amino acids 264–289; Rogers et al., 1986).

Sequences were also scanned for potential coding regions using versions 1.2 and 2 of the GRAIL neural network (data not shown). Except for *ELN* (GRAIL identified 16 of 30 exons) and *LIMK1* (15 of 16 exons), no other putative exons categorized as excellent were identified by GRAIL. GRAIL also identified 7 possible coding sequences categorized as good (6 within the 83.6 kb deletion region) and 11 categorized as marginal. All possible coding sequences classified as good were tested using either multiple-tissue Northern blot analyses or a combination of Northern blot analyses and reverse transcription–PCR (RT–PCR) of total RNA extracted from fetal and adult human brain. We found no evidence for expression of these additional possible coding sequences (data not shown).

A remarkable finding of DNA sequence analyses was the high density of Alu repetitive elements in the 83.6 kb deletion region. A total of 120 full or partial Alu sequences were identified, for an average density of ~1.4 per kilobase. A partial LINE sequence and a MER14-like element were also identified, as well as three large d(CA) repeats (Figure 2). One of the d(CA) repeats had been previously identified (Foster et al., 1993). Sequence analyses also defined the breakpoints for the K2049 deletion; both breakpoints consisted of Alu repeats, suggesting that a recombination event between these Alu sequences may have been responsible for the deletion.

LIMK1 and *ELN* Expression in the Developing Brain

To determine the expression pattern of *LIMK1*, we performed Northern blot analyses with mRNA extracted from fetal and adult tissues. A *LIMK1* oligonucleotide probe hybridized to a single mRNA of ~3.3 kb in all fetal and adult tissues examined (data not shown). Phosphorimage analyses indicated that mRNA levels varied considerably, but were highest in both fetal and adult brain. Northern blot analyses also demonstrated *LIMK1* is ubiquitously expressed in different regions of the adult human brain, with highest expression in the cerebral cortex.

In situ hybridization analyses of *LIMK1* expression in a Carnegie stage-20 (postovulatory day 50) human embryo revealed expression in the ependymal and mantle layers of the fourth ventricle, mesencephalon, and mid-area of the spinal cord (Figure 3). Additionally, *LIMK1* was expressed in the olivary nucleus, the cerebellar ependymal layer, and the peripheral nervous system, including spinal ganglia, fifth nerve ganglion, and part of the inner ear. In the spinal cord, *LIMK1* was expressed in a diffuse pattern dorsally, with ventral single-cell staining.

To determine whether *ELN* is expressed in the brain, we performed Northern blot analyses with mRNA extracted from fetal and adult tissues (data not shown). *ELN* was strongly expressed in adult heart and pancreas and in fetal lung, but exhibited negligible expression in adult and fetal brain.

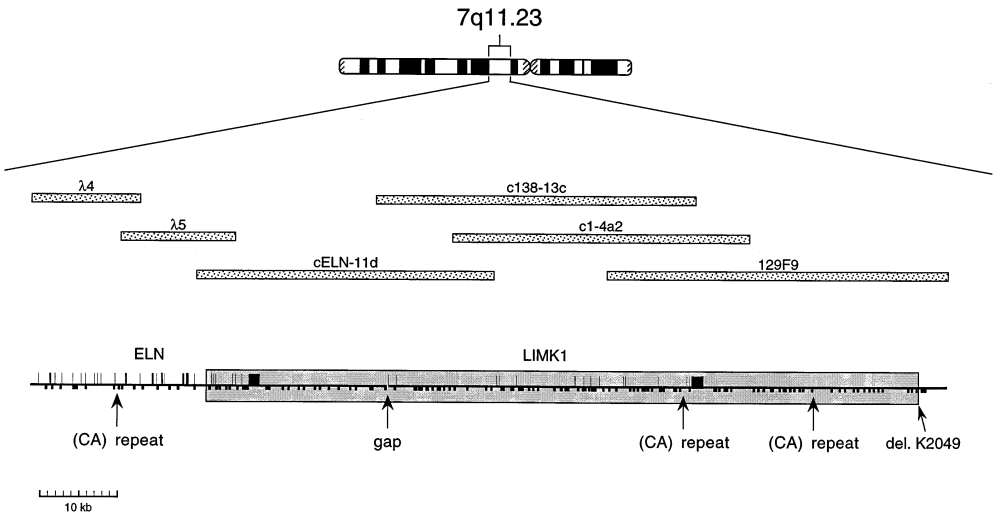

Figure 2. Physical Map of the Deletion Identified in K2049

Idiogram of chromosome 7 and a contiguous set of cosmids and phage λ from chromosome 7q11.23 that were sequenced. The relative locations and the structures of *ELN* and *LIMK1* are indicated; exons are indicated by vertical bars extending above the horizontal line; the 3′-untranslated regions of *ELN* and *LIMK1* are represented by the thick vertical bars above the line; repetitive elements (e.g., Alu repeats) are denoted by vertical bars extending below the line; the locations of three d(CA) repeats are indicated (the *ELN* d(CA) repeat has been previously defined; Foster et al., 1993). The small 250 bp gap in the sequence contig is immediately 5′ of *LIMK1*. *LIMK1* is located 15.4 kb 3′ of *ELN* and is in the same orientation. The location of the 83.6 kb deletion identified in K2049 is indicated by the long stippled box. Note that this deletion disrupts *ELN* and deletes *LIMK1*.

Discussion

We conclude that *LIMK1* hemizygosity contributes to impaired visuospatial constructive cognition in WS. This conclusion is supported by the following observations: SVAS and WSCP are coinherited in K1895 and K2049, as well as in classic WS, suggesting that the genes responsible for these two phenotypes are closely linked; *ELN* and *LIMK1* are contiguous genes that are both disrupted by an 83.6 kb deletion cosegregating with SVAS and WSCP in K2049; DNA sequence analyses of the 83.6 kb deletion region and 24 kb of flanking sequence reveal only *ELN* and *LIMK1*; *LIMK1* is highly expressed in the brain, consistent with its possible role in cognitive development; and intragenic deletions and point mutations affecting only *ELN* cause SVAS but not cognitive impairment, indicating that *ELN* hemizygosity is not sufficient to cause impaired visuospatial constructive cognition in WS.

It is also very unlikely that *ELN* mutations are necessary for impaired visuospatial constructive cognition in WS. First, no correlation exists between the severity of the vascular disease and the severity of cognitive impairment in WS. Second, ELN is a structural protein that is important for the development of elastic fibers in large arteries, lungs, and skin, but these elastic fibers are not found in the brain. Finally, ELN is not detected in neurons and glial cells of the brain (R. Mecham, personal communication). Therefore, we conclude that *ELN* mutations and secondary vascular disease are not sufficient, and almost certainly not necessary, for impaired visuospatial constructive cognition in WS.

Our conclusion that *LIMK1* hemizygosity contributes to impaired cognition would be confirmed by the identification of individuals with intragenic mutations of this gene. Preliminary experiments aimed at ascertainment of such individuals have not been successful. This is not surprising, because such individuals are probably rare and likely have a very subtle phenotype. To exclude the involvement of additional genes in development of WSCP, we sequenced the 83.6 kb deletion region and 24 kb of flanking sequence. Programs designed to identify coding regions revealed only two genes, *LIMK1* and *ELN*. While these analyses did not absolutely exclude the presence of a third gene, the sensitivity of the search algorithms was demonstrated by their identification of 15 of the 16 *LIMK1* exons. It is highly likely, therefore, that we have detected all genes in this region.

Previous studies of *LIMK1* expression are consistent with a role for this gene in cognitive development. Northern blot analyses in rat showed *LIMK1* expression in multiple tissues, with highest mRNA levels in the brain (Mizuno et al., 1994). Bernard et al. (1994) identified ubiquitous murine embryonal expression, but found significant mRNA levels only in the adult brain. In situ hybridization and immunohistochemical studies performed in mice and humans localized *LIMK1* mRNA and protein exclusively to neurons (basal ganglia, Purkinje cells, and pyramidal neurons; Bernard et al., 1994). Using Northern blot analysis, Pröschel et al. (1995) demonstrated expression of *LIMK1* in adult murine spinal cord, cortex, cerebellum, and placenta, with lower mRNA levels in several other tissues. In situ hybridization of tissues collected during various stages of murine development indicated expression of *LIMK1* in the developing brain, including the subpial layers of the frontal cortex, the midbrain roof, tectum, cerebellum, and neural epithelium of the olfactory bulb. In the adult mouse, *LIMK1* expression persisted in the cerebral cortex. Our Northern blot data indicate expression of *LIMK1* in multiple

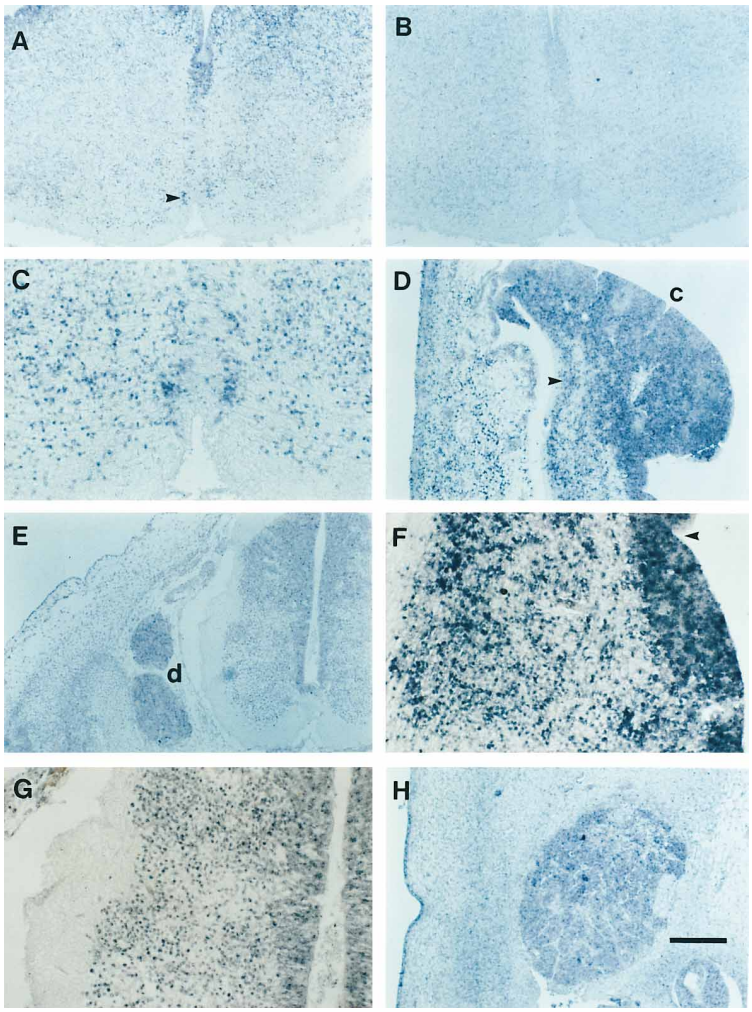

Figure 3. In Situ Hybridization Analyses of *LIMK1* Expression in the Nervous System of a Carnegie Stage-20 (50 Days Postovulatory) Human Embryo

(A) Transverse section through rhombencephalon/medulla, fourth ventricle. *LIMK1* expression is seen in the ependymal layer of the fourth ventricle, and a lower level of expression extends into the mantle layer. The arrow indicates expression in the medial accessory olivary nucleus on either side of the midline.

(B) Similar section to (A) hybridized with the sense strand cRNA probe as a negative control.

(C) Medial accessory olivary nuclei shown in the center of (A).

(D) Transverse section through the cerebellum (c) showing a high level of ependymal expression in the corpus cerebelli (fourth ventricle on the right and ectoderm on the left). Some expression is visible in the mesenchyme adjacent to the ectoderm, in particular in the presumptive dentate nucleus (arrow).

(E) Transverse section through the cervical spinal cord showing generalized expression in the dorsal (top) part of the spinal cord and single-cell staining more ventrally (right). There is also expression in the dorsal root ganglia (d).

(F) Section through the wall of the mesencephalon (the ventricle is on the far right); the ependymal layer is on the right and heavily stained, and the mantle layer in the center-left shows many cells expressing *LIMK1*. An arrow indicates the sulcus limitans.

(G) Higher magnification of (E), showing the mid-area of the spinal cord, demonstrates a low level of confluent expression in the ependymal layer (right), widespread single-cell staining in the mantle layer (center), and lack of expression in the marginal layer (left).

(H) Transverse section through the fifth nerve ganglion shows high expression in the center, in part of the inner ear (lower right, below the scale bar), and in the ectoderm (left). The scale bar represents either 100 μm (C, F, and G) or 250 μm (A, B, D, E, and H).

human fetal and adult tissues, but mRNA levels were highest in brain. In situ hybridization data presented here also indicate that in developing human tissues *LIMK1* mRNA is predominantly found in brain, a localization consistent with the pattern of *LIMK1* expression in the mouse and rat (Bernard et al., 1994; Cheng and Robertson, 1995; Nunoue et al., 1995; Pröschel et al., 1995). The discrete organization of *LIMK1* expression in the developing and adult nervous system, with consistent expression in the ependymal layer from which neurons are generated, is consistent with the hypothesis that this gene plays an important role in neural development.

Our data suggest that impaired visuospatial constructive cognition in WS results from a quantitative reduction in *LIMK1* mRNA and protein. This hypothesis is consistent with recent data examining the role of protein kinases in murine development. Impaired long-term potentiation, spatial learning, and hippocampal development were identified in mice deficient in the brain-specific protein kinases FYN (Grant et al., 1992) and the γ isoform of protein kinase C (Abeliovich et al., 1993a, 1993b). Although the spatial learning deficits observed in these mice were not directly analogous to impaired visuospatial constructive cognition in humans with WS, these data indicate a role for kinases in neuronal development.

The function of LIMK1 is not known, but the presence of specific functional domains suggests possibilities. LIM domains are zinc-binding motifs first identified in the developmentally important genes *lin-11*, *Isl-1*, and *mec-3* (Freyd et al., 1990; Karlsson et al., 1990; Way and Chalfie, 1988). LIM domains have been identified in isolation, or in combination with homeodomains, and are thought to modulate cell fate and differentiation (Schmeichel and Beckerle, 1994). LIMK1, by contrast, is unique because it contains a kinase domain in addition to two LIM domains. Predicted amino acid sequence analyses also indicate the presence of a possible PEST domain, a type of sequence often found in proteins with a short half-life. This observation suggests that levels of LIMK1 may be tightly regulated. Finally, the predicted amino acid sequence of LIMK1 indicates that cytoskeleton and nuclear localization signals may be present. Biochemical and developmental studies of LIMK1 function will be instrumental in defining the role of this protein in human cognitive development.

Our DNA sequence analyses revealed a high density of Alu repeats within the region deleted in K2049 (6-fold higher than the estimated mean density throughout the human genome; Hwu et al., 1986; Slightom et al., 1994), a density comparable with that found in the genomic region associated with DiGeorge syndrome (Budarf et al., 1995). Both WS and DiGeorge syndrome result from chromosomal rearrangements, which might be driven by the highly repetitive nature of the DNA. In this regard, it is interesting to note that we identified Alu sequences at both breakpoints in K2049, suggesting that a recombinational event between these elements may have been responsible for this deletion. Alu repeats have previously been implicated in an SVAS-associated translocation and in an intragenic deletion of *ELN* (Curran et al., 1993; Olson et al., 1995).

In summary, we have discovered that hemizygosity of *LIMK1*, a protein kinase gene expressed in the brain, likely leads to impaired visuospatial constructive cognition in WS. Further elucidation of the physiologic significance of this gene may result from gene targeting experiments in mice. Analyses of LIMK1 function should provide further insight into human cognitive development.

Experimental Procedures

Clinical Characterization of Participants

Medical records were reviewed and participants were examined by a clinical geneticist. Craniofacial features scored included dolichocephaly, broad brow, periorbital fullness, stellate iris, bitemporal narrowing, low nasal root, flat mala, full cheeks, long philtrum, small jaw, malocclusion, full nasal tip, wide mouth, full lips, prominent ear lobes, and facial asymmetry. Individuals with classic WS had $\geq$9 of the 16 features and met the diagnostic criteria of Preus (1984). The presence and extent of SVAS was determined by two-dimensional echocardiography and Doppler blood-flow analyses as described by Ensing et al. (1989). Individuals were scored as affected if there was narrowing of the ascending aorta demonstrated on echocardiography or if Doppler peak flow velocities were above normal (normal values for adults: aortic 1.0–1.7 m/s, pulmonary 0.6–0.9 m/s; for children: aortic 1.2–1.8 m/s, pulmonary 0.7–1.1 m/s). Velocities within 0.2 m/s greater than the normal range were considered weakly positive. Individuals were also scored as positive if SVAS was documented by medical records of cardiac catheterization or surgery.

Determination of WSCP

WSCP was assessed using the DAS (Elliott, 1990). The six core subtests assess language, spatial (visuospatial constructive cognition), and reasoning abilities. A diagnostic subtest measures auditory rote memory. Individuals who met one or more of the following criteria were excluded from having the WSCP:

(i) Pattern construction standard score $\geq$ mean of the core subtest scores (visuospatial constructive ability too high relative to overall level of cognitive abilities). (ii) Pattern construction standard score $\geq$ digit recall standard score (visuospatial constructive ability too high relative to auditory rote memory ability). (iii) Pattern construction standard score $\geq$ 20th percentile (absolute level of visuospatial constructive ability too high). (iv) None of the seven subtest standard scores > than 1st percentile (absolute level of ability too low).

Individuals who were not excluded were considered to have the WSCP and were evaluated further to determine the strength of their match to the WSCP. A maximum of 4 points could be earned using the following scoring system: digit recall standard score > mean of the core subtest standard scores (2 points); definitions standard score (naming vocabulary for younger children) > pattern construction standard score (1 point); similarities standard score > pattern construction standard score (1 point). Individuals obtaining a score of 4 points were considered to have an excellent fit to the WSCP, those with 3 points a very good fit, those with 2 points a good fit, and those with 0–1 point a poor fit.

The DAS was used for individuals who were at least 2.5 years old. For younger children, the WSCP was assessed using the mental scale of the Bayley (Bayley, 1969, 1993). Children who passed a greater proportion of language items attempted than nonlanguage items were considered to have the WSCP.

Individuals who did not complete the DAS were phenotypically characterized whenever possible with the WAIS-R (Wechsler, 1981) according to the following exclusion criteria: (i) block design standard score > digit span standard score; (ii) block design standard score > 20th percentile; (iii) none of the subtest standard scores > 1st percentile.

Individuals who were not excluded on the basis of these criteria were considered to have a cognitive profile consistent with the WSCP if both their digit recall and similarities standard scores were greater than their block design standard score. Those individuals who could not complete the entire WAIS-R were given the verbal portion of the WAIS-R and the VMI (Beery, 1989). Individuals were excluded from further consideration for the WSCP if their VMI age equivalent was greater than 10 years. Individuals who were not excluded were considered to have a cognitive profile consistent with the WSCP if their standard score on the verbal portion of the WAIS-R was greater than their standard score on the VMI.

Determination of Mental Retardation and Developmental Delay

Intelligence was assessed using the Bayley for children <2.5 years old, the DAS for individuals between the ages of 2.5 and 18 years, and the WAIS-R for individuals who were $\geq$18 years of age. Individuals who were at least 6 years old were considered to have mental retardation if their standard score was <70 (>2 standard deviations below the standardization sample mean). Individuals who were less than 6 years old were considered to have developmental delay if their standard score was <70.

cDNA and Genomic DNA Analyses

Genomic clones were obtained from the following sources. λ4, λ5, cELN-11d, and c138-13c were derived from primary cosmid and phage libraries constructed earlier in our laboratory (Curran et al., 1993; Ewart et al., 1994). Cosmid c1-4a2 was obtained from an amplified placental library (Stratagene). Cosmid 129F9 was isolated from the chromosome 7–specific flow-sorted cosmid library constructed at the Lawrence Livermore National Laboratories.

PCR primers were designed to amplify the region of homology in the kinase domains of PDGF receptor, HER2, HER3, FGF–FLG, FGF–BEK, insulin receptor, and IRR (sequences obtained from GenBank). The primers used were 5′-GACTTTGGGCTGGCTCGAGACA TGC-3′ and 5′-CTCCGGAGCCATCCACTTGACTGGC-3′. PCR conditions were 1 cycle of 94°C for 10 min, followed by 30 cycles of 94°C for 1 min, 49°C for 1 min, and 72°C for 1 min, ending with 1 cycle of 72°C for 10 min. Clones cELN-11d and c138-13c were used as templates. Products were cloned into pBluescript II SK(−) (Stratagene) using standard T/A cloning technology (Marchuk et al., 1991) and sequenced.

LIMK1 cDNA fragments were obtained from a human hippocampal cDNA library (Stratagene) using PCR with rTth DNA polymerase and various primers designed from the published *LIMK1* cDNA sequence (Mizuno et al., 1994). The open reading frame (*LIMK1* nucleotides 93–1936) was amplified and cloned using the following primers: 5′-ATGAGGTTGACGCTACTTTGTTGC-3′ and 5′-TCAGTCGGGGAC CTCAGGGTGGGC-3′.

FISH Analysis

FISH was performed as previously described (Curran et al., 1995). Cosmid probes c138-13c and c1-4a2 and a chromosome 7–specific marker were used as probes in these analyses.

DNA Sequence Analyses and Testing of Putative Coding Regions

Cycle sequencing of cosmids was performed using the dsDNA cycle sequencing system (GIBCO BRL) according to the instructions of the manufacturer. Addition of formamide to a final concentration of

5% allowed cycle sequencing of regions that could not be sequenced by standard conditions. Products were electrophoresed on 6% denaturing polyacrylamide gels (National Diagnostics). Sanger sequencing was performed using the Sequenase v2.0 DNA sequencing kit (United States Biochemical) according to the instructions of the manufacturer. Sequence analysis relied on the IntelliGenetics software package and BLAST (Altschul et al., 1990).

We sequenced three cosmids and two phage (λ4, λ5, cELN-11d, c1-4a2, and 129F9) that form an overlapping contig of the entire 83.6 kb deletion region in K2049 and the flanking sequences surrounding the breakpoints using the procedure described by Mardis (1994). Products from the sequencing reactions were run on either an ABI 373a Stretch DNA sequencer or an ABI 377 Prism DNA sequencer. The sequence data were processed using the XGAP algorithms (Dear and Staden, 1991, 1992). Gaps in the 83.6 kb contig were filled in by one of the following methods: direct sequencing of cosmids using specific primers; sequencing of PCR products generated using primers that flank the gaps; or subcloning restriction fragments containing the gaps into pBluescript II SK(−) (Stratagene) and sequencing them using dye primers.

The 83.6 kb sequence was analyzed using GENQUEST, BLAST, and GRAIL versions 1.2 and 2. Putative coding regions with either excellent or good scores were tested for mRNA expression by either Northern blot analysis (see below) or a combination of Northern blot analysis and RT–PCR. RT–PCR was performed according to the instructions of the manufacturer using the Thermostable rTth reverse transcriptase RNA PCR kit (Perkin Elmer). Controls included 100 ng of genomic DNA, 100 ng of genomic DNA that had been digested with 10 U of DNase I, and a water blank. RNA samples were prepared with and without DNase I treatment. Products were electrophoresed through a 5% 3:1 agarose gel (FMC) and visualized by staining with ethidium bromide.

LIMK1 and *ELN* Expression Studies

Northern blots containing ~2 μg per lane of poly(A)$^+$ mRNA were purchased from Clonetech (human MTN blot 1, human brain blots 2 and 3, and human fetal MTN blot). The blots were hybridized in ExpressHyb solution (Clonetech) according to the instructions of the manufacturer, with either ^{32}P-end-labeled *LIMK1* oligonucleotide probe (704–742 bp) or *LIMK1* (104–2038 bp), *ELN* (1–1123 bp), and β-actin cDNA clones that had been radiolabeled using random hexamer priming (Feinberg and Vogelstein, 1984). Each *LIMK1* Northern blot was analyzed by phosphorimage analyses (Molecular Dynamics) to determine the relative amounts of *LIMK1* and β-actin mRNA.

In situ hybridization was performed on 6 mm thick, paraffin-embedded sections of freshly prepared human embryos, which were obtained from the Medical Research Council–funded Human Embryonic Tissue Bank (Institute of Child Health, London). A digoxigenin-labeled 625 bp cRNA probe specific to the 3′-untranslated portion of *LIMK1* cDNA was used in these studies. Hybridization was detected by alkaline phosphatase–conjugated anti-DIG Fab fragments (Boehringer Mannheim) as previously described (Wilkinson, 1992; Birren et al., 1993). Bright-field microphotography was carried out with an Olympus BH-2 and Fujichrome 64T film.

Acknowledgments

We are grateful to the members of K2049, K1895, K1861, K2044, K1790, and K2260 and other participants in this study. We thank the Williams Syndrome Association for locating WS participants and C. Moore and D. Weaver for referring families. We appreciate the editorial assistance provided by R. Fults. M. Curran, D. Li, M. Sanguinetti, L. Urness, R. White, S. Prescott, R. Weiss, and M. Leppert offered thoughtful discussions on the manuscript. T. Fleischer provided technical assistance with the construction of cosmid maps. R. Moore and P. Thorogood (Medical Research Council, London) provided human fetal tissue samples. E. Mardis made suggestions regarding DNA sequencing. R. Shepard provided assistance with FISH analyses. G. Dalal, J. Loker, and W. Evans assisted in performing echocardiograms. Field trips were coordinated by S. Nelson and N. Cangany. We thank S. Armstrong for assistance in data collection and reduction, K. Johnson for assistance in data collection, and J. Pani for discussions of spatial cognition. This work was supported by National Heart, Lung, and Blood Institute grant R01HL4807; National Institute of Child Health and Human Development grant R01HD29957; National Institute of Neurological Disorders and Stroke grant R01NS35102; a Public Health Service research grant (M01-RR00064) from the National Center for Research Resources; a March of Dimes grant; an award from Bristol–Meyers Squibb; the Technology Access Section of the Utah Genome Center; Utah FISH and Imaging Core Facility grant 3P30 CA42014-09; and the Nevada Affiliate of the American Heart Association. N. J. G. was supported by a grant from the Wellcome Trust (035404) and by the Carrie Rudolph Trust.

Received March 25, 1996; revised June 12, 1996.

References

Abeliovich, A., Chen, C., Goda, Y., Silva, A.J., Stevens, C.F., and Tonegawa, S. (1993a). Modified hippocampal long-term potentiation in PKCγ mutant mice. Cell *75*, 1253–1262.

Abeliovich, A., Paylor, R., Chen, C., Kim, J.J., Wehner, J.M., and Tonegawa, S. (1993b). PKCγ mutant mice exhibit mild deficits in spatial and contextual learning. Cell *75*, 1263–1271.

Altschul, S.F., Gish, W., Miller, W., Myers, E.W., and Lipman, D.J. (1990). Basic local alignment search tool. J. Mol. Biol. *215*, 403–410.

Bayley, N. (1969). Bayley Scales of Infant Development (New York: Psychological Corporation).

Bayley, N. (1993). Bayley Scales of Infant Development, Second Edition (San Antonio, Texas: Psychological Corporation).

Beery, K.E. (1989). Developmental Test of Visual Motor Integration, Third Revision (Cleveland, Ohio: Modern Curriculum Press).

Bellugi, U., Wang, P.P., and Jernigan, T.L. (1994). Williams syndrome: an unusual neuropsychological profile. In Atypical Cognitive Deficits in Developmental Disorders: Implications for Brain Function, S.H. Broman and J. Grafman, eds. (Hillsdale, New Jersey: Erlbaum), pp. 23–56.

Bernard, O., Ganiatsas, S., Kannourakis, G., and Dringen, R. (1994). *Kiz-1*, a protein with LIM zinc finger and kinase domains, is expressed mainly in neurons. Cell Growth Diff. *5*, 1159–1171.

Birren, S.J., Lo, L., and Anderson, D.J. (1993). Sympathetic neuroblasts undergo a developmental switch in trophic dependence. Development *119*, 597–610.

Budarf, M.L., Collins, J., Gong, W., Roe, B., Wang, Z., Bailey, L.C., Sellinger, B., Michaud, D., Driscoll, D.A., and Emanuel, B.S. (1995). Cloning a balanced translocation associated with DiGeorge syndrome and identification of a disrupted candidate gene. Nature Genet. *10*, 269–278.

Capruso, D.X., Hamsher, K., and Benton, A.L. (1995). Assessment of visuocognitive processes. In Clinical Neuropsychological Assessment: A Cognitive Approach, R.L. Mapou and J. Spector, eds. (New York: Plenum Press), pp. 137–183.

Cheng, A.K., and Robertson, E.J. (1995). The murine LIM-kinase gene (limk) encodes a novel serine threonine kinase expressed predominantly in trophoblast giant cells and the developing nervous system. Mech. Dev. *52*, 187–197.

Curran, M.E., Atkinson, D.L., Ewart, A.K., Morris, C.A., Leppert, M.F., and Keating, M.T. (1993). The elastin gene is disrupted by a translocation associated with supravalvular aortic stenosis. Cell *73*, 159–168.

Curran, M.E., Splawski, I., Timothy, K.W., Vincent, G.M., Green, E.D., and Keating, M.T. (1995). A molecular basis for cardiac arrhythmia: *HERG* mutations cause long QT syndrome. Cell *80*, 795–803.

Dear, S., and Staden, R. (1991). A sequence assembly and editing program for efficient management of large projects. Nucl. Acids Res. *19*, 3907–3911.

Dear, S., and Staden, R. (1992). A standard file format for data from DNA sequencing instruments. DNA Seq. *3*, 99–105.

Dilts, C.V., Morris, C.A., and Leonard, C.O. (1990). Hypothesis for development of a behavioral phenotype in Williams syndrome. Am. J. Med. Genet. *6* (Suppl.), 126–131.

Elliott, C.D. (1990). Differential Ability Scales (San Diego, California: Harcourt Brace Jovanovich).

Ensing, G.J., Schmidt, M.A., Hagler, D.J., Michels, V.V., Carter, G.A., and Feldt, R.H. (1989). Spectrum of findings in a family with nonsyndromic autosomal dominant supravalvular aortic stenosis: a Doppler echocardiographic study. J. Am. Coll. Cardiol. *13*, 413–419.

Ewart, A.K., Morris, C.A., Atkinson, D.L., Jin, W., Sternes, K., Spallone, P., Stock, D., Leppert, M., and Keating, M.T. (1993a). Hemizygosity at the elastin locus in a developmental disorder, Williams syndrome. Nature Genet. *5*, 11–16.

Ewart, A.K., Morris, C.A., Ensing, G.J., Loker, J., Moore, C., Leppert, M., and Keating, M.T. (1993b). A human vascular disorder, supravalvular aortic stenosis, maps to chromosome 7. Proc. Natl. Acad. Sci. USA *90*, 3226–3230.

Ewart, A.K., Jin, W., Atkinson, D.L., Morris, C.A., and Keating, M.T. (1994). Supravalvular aortic stenosis associated with a deletion disrupting the elastin gene. J. Clin. Invest. *93*, 1071–1077.

Feinberg, A., and Vogelstein, B. (1984). A technique for radiolabeling DNA restriction endonuclease fragments to high specific activity. Anal. Biochem. *137*, 266–267.

Foster, K., Ferrell, R., King-Underwood, L., Povey, S., Attwood, J., Rennick, R., Humphries, S.E., and Henney, A.M. (1993). Description of a dinucleotide repeat polymorphism in the human elastin gene and its use to confirm assignment of the gene to chromosome 7. Ann. Hum. Genet. *57*, 87–96.

Freyd, G., Kim, S.K., and Horvitz, H.R. (1990). Novel cysteine-rich motif and homeodomain in the product of the *Caenorhabditis elegans* cell lineage gene *lin-11*. Nature *344*, 876–879.

Gilbert-Dussardier, B., Bonneau, D., Gigarel, N., Merrer, M.L., Bonnet, D., Philip, N., Serville, F., Verloes, A., Rossi, A., Ayme, S., Weissenbach, J., Mattei, M.G., Lyonnet, S., and Munnich, A. (1995). A novel microsatellite DNA marker at locus D7S1870 detects hemizygosity in 75% of individuals with Williams syndrome. Am. J. Hum. Genet. *56*, 542–544.

Grant, S.G.N., O'Dell, T.J., Karl, K.A., Stein, P.L., Soriano, P., and Kandel, E.R. (1992). Impaired long-term potentiation, spatial learning, and hippocampal development in *fyn* mutant mice. Science *258*, 1903–1910.

Hwu, H.R., Roberts, J.W., Davidson, E.H., and Britten, R.J. (1986). Insertion and/or deletion of many repeated DNA sequences in human and higher ape evolution. Proc. Natl. Acad. Sci. USA *83*, 3875–3879.

Karlsson, O., Thor, S., Norberg, T., Ohlsson, H., and Edlund, T. (1990). Insulin gene enhancer binding protein Isl-1 is a member of a novel class of proteins containing both a homeo and a Cys-His domain. Nature *344*, 879–882.

Lowery, M.C., Morris, C.A., Ewart, A., Brothman, L.J., Zhu, X.L., Leonard, C.O., Carey, J.C., Keating, M., and Brothman, A.R. (1995). Strong correlation of elastin deletions, detected by FISH, with Williams syndrome: evaluation of 235 patients. Am. J. Hum. Genet. *57*, 49–53.

Marchuk, D., Drumm, M., Saulino, A., and Collins, F.S. (1991). Construction of T-vectors, a rapid and general system for direct cloning of unmodified PCR products. Nucl. Acids Res. *19*, 1154.

Mardis, E.R. (1994). High-throughput detergent extraction of M13 subclones for fluorescent DNA sequencing. Nucl. Acids Res. *22*, 2173–2175.

Mervis, C.B., and Bertrand, J. (1996). Relations between cognition and language: a developmental perspective. In Research on Communication and Language Disorders: Contributions to Theories of Language Development, L.B. Adamson and M.A. Romski, eds. (New York: Brookes), in press.

Mervis, C.B., Morris, C.A., Bertrand, J., and Robinson, B.F. (1996). Williams syndrome: findings from an integrated program of research. In Neurodevelopmental Disorders: Contributions to a New Framework from the Cognitive Neurosciences, H. Tager-Flusberg, ed. (Cambridge, Massachusetts: MIT Press), in press.

Mizuno, K., Okano, I., Ohashi, K., Nunoue, K., Kuma, K., Miyata, T., and Nakamura, T. (1994). Identification of a human cDNA encoding a novel protein kinase with two repeats of the LIM/double zinc finger motif. Oncogene *9*, 1605–1612.

Morris, C.A., Dilts, C., Demsey, S.A., Leonard, C.O., and Blackburn, B. (1988). The natural history of Williams syndrome: physical characteristics. J. Pediatr. *113*, 318–326.

Morris, C.A., Loker, J., Ensing, G., and Stock, A.D. (1993). Supravalvular aortic stenosis cosegregates with a familial 6;7 translocation which disrupts the elastin gene. Am. J. Med. Genet. *46*, 737–744.

Nunoue, K., Ohashi, K., Okano, I., and Mizuno, K. (1995). LIMK-1 and LIMK-2, two members of a LIM motif-containing protein kinase family. Oncogene *11*, 701–710.

Olson, T.M., Michels, V.V., Urban, Z., Csiszar, K., Christiano, A.M., Driscoll, D.J., Feldt, R.H., Boyd, C.D., and Thibodeau, S.N. (1995). A 30 kb deletion within the elastin gene results in familial supravalvular aortic stenosis. Hum. Mol. Genet. *4*, 1677–1679.

Ponting, C.P., and Phillips, C. (1995). DHR domains in syntrophins, neuronal NO synthases and other intracellular proteins. Trends Biochem. Sci. *20*, 102–103.

Preus, M. (1984). The Williams syndrome: objective definition and diagnosis. Clin. Genet. *25*, 422–428.

Pröschel, C., Blouin, M.-J., Gutowski, N.J., Ludwig, R., and Noble, M. (1995). Limk1 is predominantly expressed in neural tissues and phosphorylates serine, threonine and tyrosine residues *in vitro*. Oncogene *11*, 1271–1281.

Rogers, S., Wells, R., and Rechsteiner, M. (1986). Amino acid sequences common to rapidly degraded proteins: the PEST hypothesis. Science *234*, 364–368.

Schmeichel, K.L., and Beckerle, M.C. (1994). The LIM domain is a modular protein-binding interface. Cell *79*, 211–219.

Slightom, J.L., Siemieniak, D.R., Sieu, L.C., Koop, B.F., and Hood, L. (1994). Nucleotide sequence of 77.7 kb of the human V_β T-cell receptor gene locus: direct primer-walking using cosmid template DNAs. Genomics *20*, 149–168.

Udwin, O., Yule, W., and Martin, N. (1987). Cognitive abilities and behavioral characteristics of children with idiopathic infantile hypercalcemia. J. Child Psychol. Psychiatry *28*, 297–309.

Way, J.C., and Chalfie, M. (1988). *mec-3*, a homeobox-containing gene that specifies differentiation of the touch receptor neurons in C. elegans. Cell *54*, 5–16.

Wechsler, D. (1981). Wechsler Adult Intelligence Scale-Revised (San Antonio, Texas: Psychological Corporation).

Wilkinson, D.G. (1992). *In Situ* Hybridisation: A Practical Approach (Oxford: IRL Press).

Xu, Y., Einstein, J.R., Mural, R.J., Shah, M.B., and Uberbacher, E.C. (1994). An improved system for exon recognition and gene modeling in human DNA sequences. In Proceedings of the Second International Conference on Intelligent Systems for Molecular Biology, R. Altman, ed. (Menlo Park, California: American Association for Artificial Intelligence Press), pp. 376–384.

GenBank Accession Numbers

The accession numbers for the sequences of the contigs containing the *ELN* and *LIMK1* genes are U62292 and U62293, respectively.